

# Cramer-Rao Bound for Indoor Visible Light Positioning Using an Aperture-Based Angular-Diversity Receiver

Heidi Steendam\*, Thomas Q. Wang<sup>†</sup>, Jean Armstrong<sup>†</sup>

\* Department of Telecommunications and Information Processing, Ghent University, Ghent, Belgium,  
Email: Heidi.Steendam@ugent.be

<sup>†</sup> Department of Electrical and Computer Systems Engineering, Monash University, Melbourne, Australia,  
Email: {Tom.Wang, Jean.Armstrong}@monash.edu

**Abstract**—In this paper, we investigate the problem of indoor positioning using visible light systems. The directional detector array we use is comprised of a number of receiving elements, each consisting of an aperture and a photo diode, which are arranged to offer good angular diversity, and can be implemented within a compact receiver structure [1]. The receiving elements receive the light from a number of white LEDs, which are typically attached to the ceiling, and which act as anchors. In order to get an indication of the received signal strengths of the different LEDs, we average the received signals over time. The relative signal strengths in the different receiving elements do not only provide information on the distance between the LEDs and the detector array, but also about the angle-of-arrival of the light. By combining the information of the receiving elements, the position of the detector can be estimated. In order to assess the accuracy of positioning algorithms based on this approach, we derive the Cramer-Rao lower bound on the position accuracy. Assuming the white LEDs transmit an optical power of 1 W, and the time averaging is done over 1 millisecond, an accuracy of the order of a centimetre can be achieved.

## I. INTRODUCTION

Many current and next-generation applications in automotive, military and public service systems require accurate estimates of the position of an object or a person. Although GPS technology offers a rough position estimate, which is sufficient for many outdoor applications, this technology can often not be applied indoors because of reduced satellite reception. Many solutions for indoor positioning have been investigated during the last decade [2]-[4]. However, an accurate, low-cost, low-power solution for indoor positioning is still lacking.

Recently, indoor positioning based on the reception of visible light has become an important research topic [5]. Due to their energy efficiency, white LEDs are gradually replacing conventional fluorescent and incandescent lights. As, unlike conventional light sources, these LEDs can easily be modulated, white LEDs have been considered for high speed data transmission [6], and recently also for positioning [7]-[13]. Compared to RF positioning solutions, positioning based on visible light has a number of advantages. Almost every indoor area needs some kind of illumination, so by combining it with communication and positioning, the overall deployment cost is reduced compared to the case where illumination,

communication and positioning are provided by separate systems. Further, as the luminaries are generally placed at regular intervals on the ceiling, they have LOS to most positions in the room. Moreover, interference with signals from other rooms is absent as light is blocked by opaque walls. These features make white LEDs a viable candidate for a low-cost positioning system, and several solutions have been proposed to estimate a position using white LEDs [5].

As in RF positioning, different approaches exist. These can be classified according to i) the parameters that are estimated to find the position, and ii) the type of detector used. Firstly, regarding the parameters that are estimated, most papers deal with a two-step approach, where e.g. first the distance between the LED and the detector is estimated based on RSS [9]-[11], TOA [7], angle-of-arrival (AOA) [12] or phase difference of arrival (PDOA) [8], and then based on the distance (or angle) the position is estimated using trilateration or triangulation. Besides the two-step approaches, direct estimation of the position is possible, e.g. [13] directly estimates the detector's position from the received signal, by discretising the possible position estimates. This latter approach theoretically offers a higher accuracy and suffers less from ambiguities, although the resulting position estimation algorithm in general will have a higher complexity than the two-step approaches. Secondly, with regard to the detector used, we distinguish the solutions that apply a CCD sensor [14] and those which use photo diodes (PDs) [7]-[13]. A CCD sensor has a large number of pixels so that one sensor offers a large number of observations, which makes it suitable for accurate AOA estimation. However, CCD sensors have a slow response time and are energy inefficient. On the other hand, PDs are energy efficient and have a faster response. By combining a PD with a lens or an aperture, directional information can be extracted from the incoming light.

Although the optical positioning papers show that accurate position estimates are possible using white LEDs, research on the theoretical limits on the estimation errors is mostly lacking. To be able to optimize the system parameters to achieve optimal accuracy, knowledge of the theoretical limits such as the Cramer-Rao bound (CRB), which is a lower bound

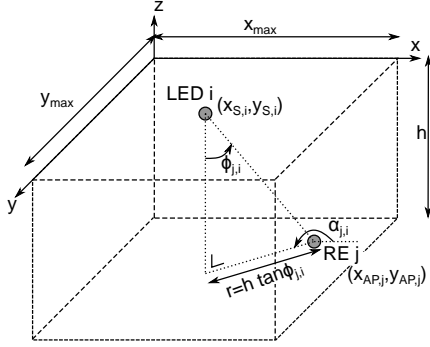


Fig. 1. View of the room and the positions of LED  $i$  and RE  $j$ .

on the mean-squared estimation error of an unbiased estimate, is of utmost importance. This CRB not only depends on the type of parameters which are detected, but also on the type of detector which is considered. In the literature, only a few papers deal with the CRB for visible light positioning using PDs [15]-[17]. The authors in [15] consider a two-step approach, where the distance between the LEDs and the detector is estimated based on the RSS, and the position is estimated by trilateration. However, results are only given for the case where the detectors are perfectly oriented towards the LEDs, and the Lambertian order of the LEDs ranges in the interval [30, 80] making the light beam transmitted by the LED extremely narrow. Similarly as in [15], the authors in [16] use directional LEDs and an unidirectional receiver, but they consider hybrid RSS and AOA positioning. In [17], the CRB is considered for the TOA approach, assuming the detector is comprised of bare photo diodes (PD). The resulting CRB promises centimetre accuracy for realistic scenarios, although this approach requires accurate synchronisation of the signals.

In this paper, we consider the CRB for direct estimation of the position from the detected optical signals, using non-directional LEDs and the directional receiver proposed in [1]. We average over time the signals at the output of the PDs in the different receiving elements of the detector array in order to gather position-related information. The resulting observations not only contain information about the distance between the LED and the detector array, but also about the angle-of-arrival (AOA). Using this information, we directly determine the position of the detector array<sup>1</sup>. The resulting accuracy is of the order of a centimetre, e.g. for LEDs transmitting 1 W optical power and an averaging time of 1 ms, an accuracy of a centimetre can be obtained.

## II. SYSTEM DESCRIPTION

### A. Received Signals

We consider a configuration where  $K$  LEDs are attached to the ceiling of the room at positions  $(x_{S,i}, y_{S,i})$ ,  $i = 1, \dots, K$ . The detector array is located at a distance  $h$  below the ceiling,

<sup>1</sup>Hence, we do not consider a two-step approach where first the RSS or AOA is estimated, and then the position is estimated using trilateration or triangulation.

as shown in Figure 1. The detector array consists of  $M$  receiving elements (RE), each consisting of a bare PD and an aperture (see Figure 2a). The aperture is a circular hole in an opaque screen at height  $r$  above the detecting plane of the PD, and the position of the centre of the aperture  $j$  is given by  $(x_{AP,j}, y_{AP,j})$ ,  $j = 1, \dots, M$ . We assume that the only light that reaches a PD is that passing through its aperture. We denote the radius of the aperture and the PD as  $R_A$  and  $R_D$ , respectively. Further, assuming that the RE is in the far field of the LED and the size of the aperture is large compared with the wavelength of the light, the light from a LED will result in a circle on the detecting plane (Figure 2b). In the following, we assume that  $r = R_A = R_D$ , as in that case, the sizes of the light spot and the PD are equal, so a small change in the detector array position will always result in different signal strengths at the output of each PD. In order to extract the position of the detector array from the received signals, we describe the signals reaching the detector array as functions of the incident and polar angles  $(\phi_{j,i}, \alpha_{j,i})$  between LED  $i$  and RE  $j$ . The relationship between the coordinates  $(x_{S,i}, y_{S,i})$  and  $(x_{AP,j}, y_{AP,j})$  of LED  $i$  and aperture  $j$ , respectively, and the incident and polar angles  $(\phi_{j,i}, \alpha_{j,i})$  is given by

$$\begin{aligned} x_{S,i} &= x_{AP,j} + h \tan \phi_{j,i} \cos \alpha_{j,i} \\ y_{S,i} &= y_{AP,j} + h \tan \phi_{j,i} \sin \alpha_{j,i}. \end{aligned} \quad (1)$$

Further, the positions of the apertures with respect to the position  $(x_U, y_U)$  of the detector array are given by  $(x_{AP,j}, y_{AP,j}) = (x_U + \delta x_j, y_U + \delta y_j)$ , where  $(\delta x_j, \delta y_j)$  is determined by the layout of the detector array. In order to achieve angular diversity from the detector array, the PDs are slightly shifted relative to their apertures. The relative position of PD  $j$  with respect to its aperture is determined by the polar angle  $\alpha_{AP,j}$  and the distance  $d_{AP,j}$  between the centres of the aperture and the PD.

We assume that the LEDs are generalized Lambertian LEDs with order  $m$ . Further, denote  $s_i(t)$  as the optical signal transmitted by LED  $i$ . We assume the receiver can distinguish the signals from the different LEDs. This could be achieved by transmitting the signals in different time slots. At the output of the PDs, we take the time-average of the electrical signal over the interval  $[0, T]$ :  $r_j = \frac{1}{T} \int_0^T r_j(t) dt$ . The resulting observation  $\mathbf{r}$  is given by

$$\mathbf{r} = R_p \mathbf{H} \mathbf{s} + \mathbf{n}, \quad (2)$$

where  $\mathbf{r} = (r_1 \dots r_M)^T$ ,  $\mathbf{s} = (s_1 \dots s_K)^T$  with  $s_i = \frac{1}{T} \int_0^T s_i(t) dt$  is the optical power transmitted by LED  $i$ ,  $R_p$  is the responsivity of the PD,  $\mathbf{H}$  is the channel gain matrix with  $(\mathbf{H})_{j,i} = h_c^{(j,i)}$  and  $\mathbf{n}$  is shot noise. This shot noise can be modelled as i.i.d. zero-mean Gaussian random variables with variance  $N_0/2T$  with  $N_0 = 2qR_p p_n A_D \Delta \lambda$ , where  $q$  is the charge of an electron,  $p_n$  is the background spectral irradiance,  $A_D$  is the surface of the PD and  $\Delta \lambda$  is the bandwidth of the optical filter in front of the PD. Further, the channel gain  $h_c^{(j,i)}$  can be written as

$$h_c^{(j,i)} = \frac{m+1}{2\pi h^2} A_0^{(j,i)} \cos^{m+3} \phi_{j,i} \quad (3)$$

where  $A_0^{(j,i)}$  is the surface of the overlap area between PD  $j$  and the light spot originating from LED  $i$  [1]:

$$A_0^{(j,i)} = \begin{cases} 2R_D^2 \arccos\left(\frac{d_{j,i}}{2R_D}\right) & 0 \leq d_{j,i} \leq 2R_D \\ -\frac{d_{j,i}}{2} \sqrt{4R_D^2 - d_{j,i}^2} & \\ 0 & d_{j,i} > 2R_D \end{cases}. \quad (4)$$

The distance  $d_{j,i}$  between the centre of the light spot and the centre of the PD is given by

$$\begin{aligned} d_{j,i} &= \left[ \left( d_S^{(j,i)} \cos \alpha_S^{(j,i)} - d_{AP,j} \cos \alpha_{AP,j} \right)^2 \right. \\ &\quad \left. + \left( d_S^{(j,i)} \sin \alpha_S^{(j,i)} - d_{AP,j} \sin \alpha_{AP,j} \right)^2 \right]^{1/2} \\ &= \left[ \left( -\frac{R_D}{h} (x_{S,i} - x_{AP_j}) - d_{AP,j} \cos \alpha_{AP,j} \right)^2 \right. \\ &\quad \left. + \left( -\frac{R_D}{h} (y_{S,i} - y_{AP_j}) - d_{AP,j} \sin \alpha_{AP,j} \right)^2 \right]^{1/2} \end{aligned} \quad (5)$$

with  $d_S^{(j,i)} = R_D \tan \phi_{j,i}$  and  $\alpha_S^{(j,i)} = \pi + \alpha_{j,i}$ , and the second line in (5) is obtained by substituting (1).

### B. Cramer-Rao Bound

We now derive the CRB for the estimate of the position  $\boldsymbol{\theta} = (x_U, y_U)$  of the detector array based on the observation (2). The mean-squared error of any unbiased estimate  $\hat{\boldsymbol{\theta}} = (\hat{x}_U, \hat{y}_U)$  of the position  $\boldsymbol{\theta} = (x_U, y_U)$ , i.e.,  $\text{MSE} = E[(x_U - \hat{x}_U)^2 + (y_U - \hat{y}_U)^2]$ , is lower bounded by

$$\text{MSE} \geq \text{trace}(\mathbf{F}_U^{-1}) \quad (6)$$

where  $\mathbf{F}_U$  is the Fisher information matrix (FIM) [18], defined as

$$\mathbf{F}_U = E \left[ (\nabla_{\boldsymbol{\theta}} \ln p(\mathbf{r}|\boldsymbol{\theta})) (\nabla_{\boldsymbol{\theta}} \ln p(\mathbf{r}|\boldsymbol{\theta}))^T \right]. \quad (7)$$

Taking into account that  $\mathbf{r}$  given  $\boldsymbol{\theta}$  is Gaussian distributed with mean  $R_p \mathbf{H} \mathbf{s}$  and autocorrelation matrix  $\frac{N_0}{2T} \mathbf{I}_M$ , where  $\mathbf{I}_M$  is the  $M \times M$  identity matrix, i.e.,  $\mathbf{r}|\boldsymbol{\theta} \sim N(R_p \mathbf{H} \mathbf{s}, \frac{N_0}{2T} \mathbf{I}_M)$ , the FIM can be rewritten as

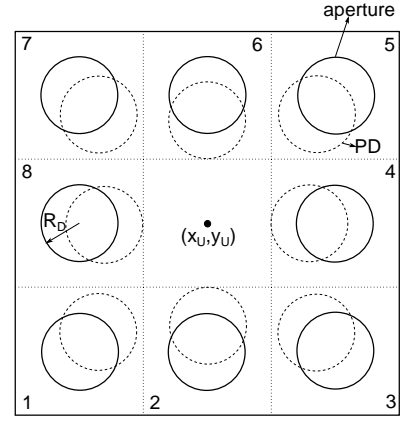
$$\mathbf{F}_U = \frac{2TR_p^2}{N_0} \begin{bmatrix} \mathbf{s}^T \mathbf{X}^{x_U, x_U} \mathbf{s} & \mathbf{s}^T \mathbf{X}^{x_U, y_U} \mathbf{s} \\ \mathbf{s}^T \mathbf{X}^{y_U, x_U} \mathbf{s} & \mathbf{s}^T \mathbf{X}^{y_U, y_U} \mathbf{s} \end{bmatrix}, \quad (8)$$

where  $(\mathbf{X}^{a,b})_{i,i'}$ ,  $a, b \in \{x_U, y_U\}$  is defined as

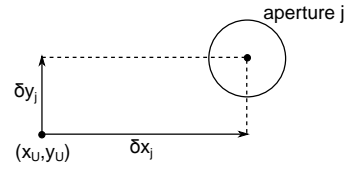
$$\begin{aligned} (\mathbf{X}^{ab})_{i,i'} &= \left[ \left( \frac{\partial}{\partial a} \mathbf{H} \right)^T \left( \frac{\partial}{\partial b} \mathbf{H} \right) \right]_{i,i'} \\ &= \sum_{j=1}^M \frac{\partial}{\partial a} h_c^{(j,i)} \frac{\partial}{\partial b} h_c^{(j,i')}. \end{aligned} \quad (9)$$

The derivative of the channel gain  $h_c^{(j,i)}$  (3) with respect to  $x_U$  and  $y_U$  can be written as

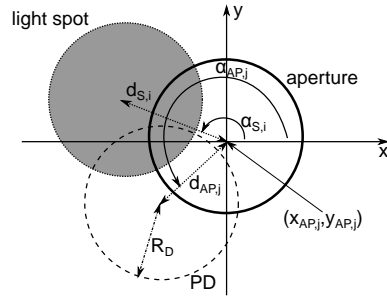
$$\begin{aligned} \frac{\partial}{\partial a} h_c^{(j,i)} &= \frac{m+1}{2\pi h^2} \left[ \left( \frac{\partial}{\partial a} A_0^{(j,i)} \right) \cos^{m+3} \phi_{j,i} \right. \\ &\quad \left. + A_0^{(j,i)} \frac{\partial}{\partial a} \cos^{m+3} \phi_{j,i} \right] \end{aligned} \quad (10)$$



(a)



(b)



(c)

Fig. 2. a) Top view of a detector array structure consisting of  $M = 8$  REs, b) relative position of aperture  $j$  with respect to the reference position  $(x_U, y_U)$  and c) top view of one RE.

with  $a \in \{x_U, y_U\}$ . Taking into account (1), (4) and (5), it follows that

$$\begin{aligned} \frac{\partial}{\partial x_U} \cos^{m+3} \phi_{j,i} &= \frac{m+3}{h^2} (x_{S,i} - x_{AP,j}) \cos^{m+5} \phi_{j,i} \\ \frac{\partial}{\partial y_U} \cos^{m+3} \phi_{j,i} &= \frac{m+3}{h^2} (y_{S,i} - y_{AP,j}) \cos^{m+5} \phi_{j,i}. \end{aligned} \quad (11)$$

For  $0 \leq d_{j,i} \leq 2R_D$  and  $a \in \{x_U, y_U\}$ ,  $\frac{\partial}{\partial a} A_0^{(j,i)}$  yields

$$\frac{\partial}{\partial a} A_0^{(j,i)} = -\sqrt{4R_D^2 - d_{j,i}^2} \frac{\partial}{\partial a} d_{j,i} \quad (12)$$

and

$$\begin{aligned}\frac{\partial}{\partial x_U} d_{j,i} &= -\frac{R_D}{hd_{j,i}} \left( \frac{R_D}{h} (x_{S,i} - x_{AP,j}) \right. \\ &\quad \left. + d_{AP,j} \cos \alpha_{AP,j} \right) \\ \frac{\partial}{\partial y_U} d_{j,i} &= -\frac{R_D}{hd_{j,i}} \left( \frac{R_D}{h} (y_{S,i} - y_{AP,j}) \right. \\ &\quad \left. + d_{AP,j} \sin \alpha_{AP,j} \right).\end{aligned}\quad (13)$$

With the general expression (8), the lower bound on the MSE (6) can be computed for any optical signal  $s_i(t)$  and different transmitted optical powers  $s_i$ . Further, as (8) is a function of the positions of the apertures  $(x_{AP,j}, y_{AP,j})$  and the positions of the corresponding PDs  $(d_{AP,j}, \alpha_{AP,j})$ , the expression can be used to investigate the influence of the detector array layout.

In the special case where all transmitted optical powers are equal, i.e.,  $s_i = P_{opt}$ , the FIM reduces to

$$\mathbf{F}_U = T \frac{2P_{opt}^2 R_p^2}{N_0} \sum_{i,i'=1}^K \begin{bmatrix} \mathbf{X}_{i,i'}^{x_U, x_U} & \mathbf{X}_{i,i'}^{x_U, y_U} \\ \mathbf{X}_{i,i'}^{y_U, x_U} & \mathbf{X}_{i,i'}^{y_U, y_U} \end{bmatrix}, \quad (14)$$

in other words, the CRB is inversely proportional to the ratio  $\gamma = 2P_{opt}^2 R_p^2 / N_0$  and the time interval  $T$ . This ratio  $\gamma$  is related to the SNR, which is defined as the received useful power compared to the receiver noise power, i.e.,  $\text{SNR} = 2P_{opt}^2 (h_c^{(j,i)})^2 R_p^2 / N_0$ . Assuming  $m = 1$ ,  $A_0 = \pi R_D^2$  with  $R_D = 1$  mm,  $\cos \phi_{j,i} = 1$  and  $h = 2$  m in (3), the difference between the ratio  $\gamma$  and the SNR is 132.04 dB. This large channel loss is due to the characteristics of the optical channel. From (14) it follows that, by increasing the length  $T$  of the time-averaging, we can improve the accuracy of the positioning.

### III. NUMERICAL RESULTS

In this section, we evaluate the CRB derived in the previous section for the detector array structure shown in Figure 2a, with  $M = 8$  REs. In the simulations, we assume the relative positions  $(\delta x_j, \delta y_j)$  of the apertures with respect to the position  $(x_U, y_U)$  of the detector array are given by  $\delta_{\mathbf{x}} = \epsilon R_D (-1 \ 0 \ 1 \ 1 \ 1 \ 0 \ -1 \ -1)$  and  $\delta_{\mathbf{y}} = \epsilon R_D (-1 \ -1 \ -1 \ 0 \ 1 \ 1 \ 1 \ 0)$ , with  $\epsilon = 5$  and  $R_D = 1$  mm. However, simulation results not shown in this paper, reveal that neither the distance  $\epsilon$  nor a rotation of the detector array in the  $(x, y)$ -plane will have a significant influence on the CRB. Further, the positions of the PDs relative to their apertures are given by  $d_{AP,j} = \zeta R_D$  and  $\alpha_{AP,j} = j \frac{\pi}{4}$ . We assume that the detector array is positioned parallel to the ceiling, i.e. the plane where the LEDs are positioned. The LEDs are Lambertian with order  $m = 1$ , which corresponds to a non-directional radiation pattern. We consider in our results two possible configurations of the LEDs, one with  $K = 4$  LEDs at positions  $\mathbf{x}_S = \frac{x_{\max}}{4} (1 \ 3 \ 1 \ 3)$  and  $\mathbf{y}_S = \frac{y_{\max}}{4} (1 \ 1 \ 3 \ 3)$ , and one with  $K = 16$  LEDs at positions  $\mathbf{x}_S = \frac{x_{\max}}{8} (1 \ 3 \ 5 \ 7 \ 1 \ 3 \ 5 \ 7 \ 1 \ 3 \ 5 \ 7 \ 1 \ 3 \ 5 \ 7)$  and  $\mathbf{y}_S = \frac{y_{\max}}{8} (1 \ 1 \ 1 \ 1 \ 3 \ 3 \ 3 \ 3 \ 5 \ 5 \ 5 \ 5 \ 7 \ 7 \ 7 \ 7)$ , where  $x_{\max} = 10$  m and  $y_{\max} = 10$  m are the length and width of the room, and the plane of the detector array is at a distance

$h = 2$  m below the ceiling. We assume the background spectral irradiance equals  $p_n = 5.8 \times 10^{-6}$  W/cm<sup>2</sup>·nm, which is a value that is often considered in the literature [19]. The PD has a responsivity  $R_p = 0.4$  mA/mW [20] and the bandwidth  $\Delta\lambda$  of the optical filter equals 360 nm (from 380 to 740 nm). Assuming the radius of the PD equals  $R_D = 1$  mm, the one-sided noise spectral density equals  $N_0 = 8.4 \times 10^{-24}$  A<sup>2</sup>/Hz, which corresponds to  $\gamma = 225.8$  dB.

In Figure 3, we show the square root of the CRB as a function of the position  $(x_U, y_U)$  of the detector array in the room, assuming the received signal is averaged over  $T = 1$  ms and  $T = 0.1$  ms for  $K = 4$  and  $K = 16$ , which correspond to  $T\gamma = 195.8$  dB and  $T\gamma = 185.8$  dB, respectively. As can be observed, the root of the CRB (rCRB) is a function of the position of the detector array: for most of the room, the rCRB is relatively constant, only near the walls, the rCRB increases. This can be explained as near the walls, less light reaches the detector array because of the radiation pattern of the LEDs and the directionality of the different REs in the detector array [1]. Further, we compute the spatial average of the rCRB, i.e., the average of the rCRB over all positions in the room. The value of  $\text{rCRB}_{\text{av}}$  is indicated in Figure 3 for all the cases considered. It can be observed that the position accuracy that can be obtained improves when the time interval  $T$  increases, because of the noise averaging. Further, by increasing the number of LEDs from 4 to 16, the accuracy improves by about 45%. For all cases considered in Figure 3, a positioning accuracy of the order of a centimetre is obtained.

Next, we evaluate the spatial average of the rCRB as function of the time interval  $T$  of the time-averaging (see Figure 4). As expected from (14), the average rCRB improves according to the square root of  $T$ . The figure reveals that when the time window is larger than 1 ms, an accuracy less than 1 cm can be obtained. Hence, real-time accurate position estimates are achievable using the proposed approach.

To evaluate the influence of the layout of the detector array, we show the dependency of the spatial average of the rCRB on the distance  $\zeta R_D$  between a PD and its aperture in Figure 5. We observe that for small values of  $\zeta$ ,  $\text{rCRB}_{\text{av}}$  reduces as function of  $\zeta$ , whereas for larger  $\zeta$ ,  $\text{rCRB}_{\text{av}}$  is an increasing function of  $\zeta$ . This can be explained as follows. For small values of  $\zeta$ , all REs will approximately receive the same amount of light, irrespective of the position of the detector array. Hence, the detector array is less able to extract information about the polar angle, i.e. the detector array does not offer sufficient angular diversity. By increasing  $\zeta$ , the angular diversity of the detector array improves. However, if  $\zeta$  is too large, because of the directionality of the REs, less light will reach the PDs for most of the positions in the room, so that the accuracy will reduce. As can be observed in Figure 5, the optimal value of  $\zeta$  is in the range [0.5, 1.5].

Finally, in Figure 6, the spatial average of the rCRB is plotted as function of the radius of the PD. The rCRB improves approximately in inverse proportion to the radius  $R_D$  of the PD, or in other words, with the square root of the area of the PD. This can be explained by inspecting (3), (4) and (5):

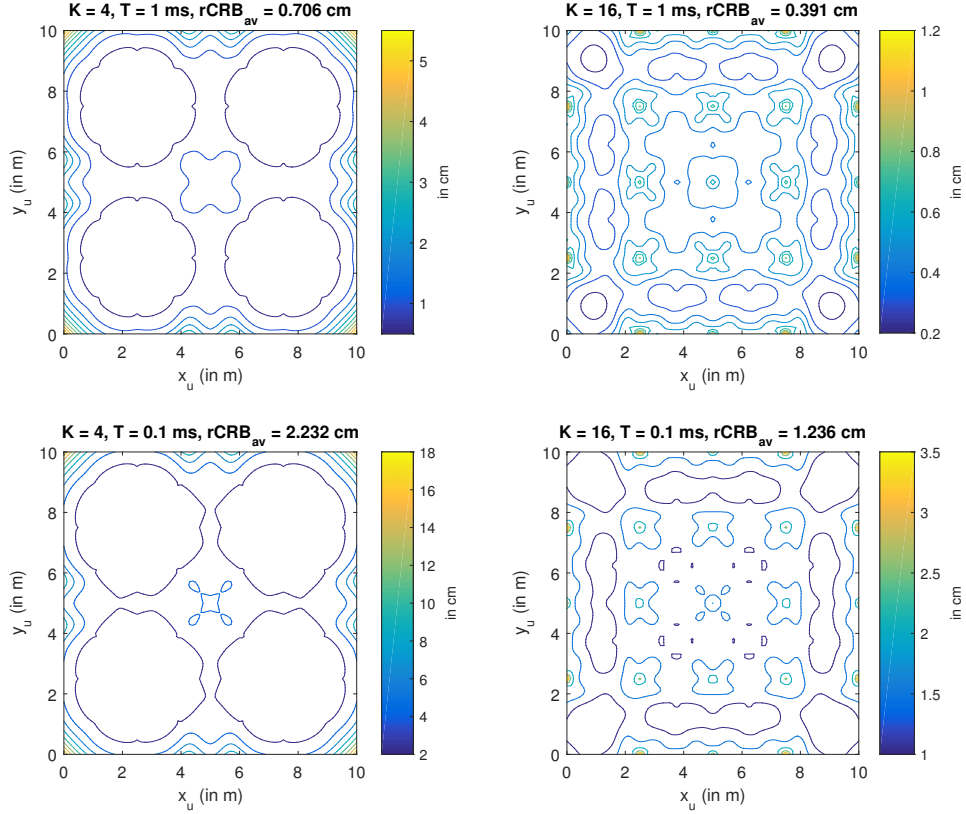


Fig. 3. Square root of the CRB as function of the position  $(x_U, y_U)$  of the detector array in the room, for  $\zeta = 1$  and  $R_D = 1$  mm.

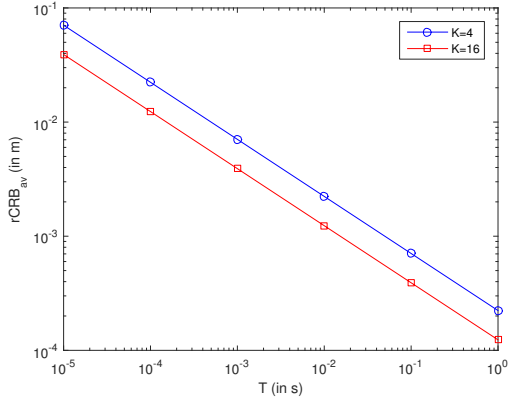


Fig. 4. Spatial average of rCRB as function of the averaging interval  $T$ , for  $\zeta = 1$ ,  $R_D = 1$  mm.

the channel gain  $h_c^{(j,i)}$  only depends on  $R_D$  through  $A_0^{(j,i)}$ , which is proportional to  $R_D^2$ . Hence, the elements of  $\mathbf{X}^{a,b}$  are essentially proportional to  $R_D^4$ . On the other hand, the noise level  $N_0$  is proportional to  $R_D^2$  through the surface  $A_D$  of the PD. Consequently, the FIM will be proportional to  $R_D^2$ .

#### IV. CONCLUSIONS

In this paper, we investigate visible light positioning using a directional detector array that is comprised of a number of receiving elements, each consisting of an aperture and a bare photo diode, to collect the incident light. The apertures and

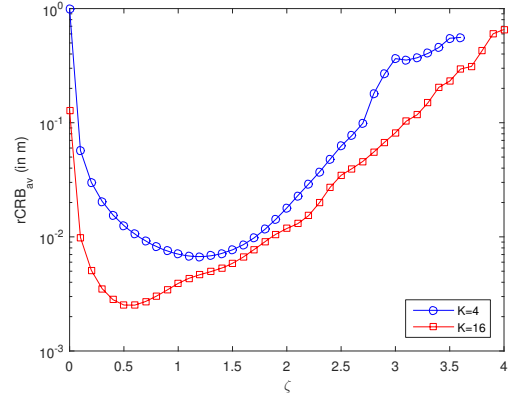


Fig. 5. Spatial average of rCRB as function of the distance  $\zeta R_D$  between the PD and its aperture, for  $T = 1$  ms,  $R_D = 1$  mm.

photo diodes are placed to have angular diversity and still have a large field-of-view. This property of the detector array allows more directional information to be extracted from the light than when using a single photo diode, as proposed in [16]. The signals at the different photo diodes of the detector array are averaged over a time window  $T$  in order to obtain information about the incident optical power. Based on the resulting observations, we derive the Cramer-Rao bound for direct estimation of the detector array's position.

As shown in the paper, the accuracy of positioning is determined by the duration of the time window  $T$ . We show

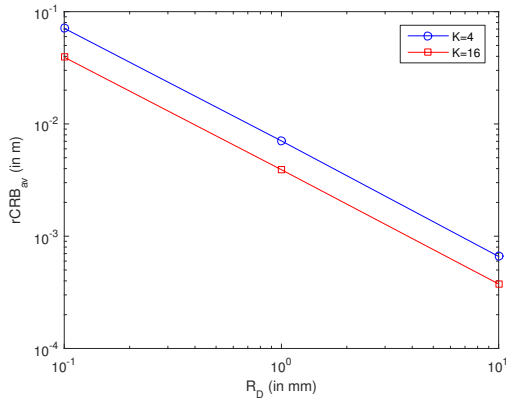


Fig. 6. Spatial average of rCRB as function of the radius  $R_D$  of the PD,  $T = 1$  ms,  $\zeta = 1$ .

that, for a time interval of 1 ms, the accuracy is of the order of a centimetre, which is at least an order of magnitude lower than positioning based on RSS measurements using WiFi or BLE, and of the same order of accuracy as obtained with UWB signals. In order to obtain this accuracy, we considered the time-averaging over a time interval of the order of a millisecond. As the optical channel is very stable and only changes slowly as a function of time, this is a realistic assumption. Hence, taking into account that with the proposed approach, real-time accurate positioning is achievable, at a deployment cost that is low compared to UWB systems, positioning using visible light is a formidable alternative for indoor positioning.

Although the results of this paper promise an accuracy of the order of a centimetre, in reality the accuracy will be degraded by system imperfections, such as the differences in DC offsets at the transmitters and receiver, imperfections in the sizes and shapes of the PDs and apertures, and reflections of the transmitted light on walls. However, it is expected that the resulting accuracy is still better than WiFi or BLE, and of the same order of magnitude of UWB suffering from imperfections such as multipath interference.

#### ACKNOWLEDGEMENT

Heidi Steendam gratefully acknowledges the financial support from the Flemish Fund for Scientific Research (FWO). This research has been funded by the Interuniversity Attraction Poles Programme initiated by the Belgian Science Policy Office. This research was carried out during the sabbatical leave of Heidi Steendam at Monash University. This work was supported by the Australian research Council's (ARC) Discovery funding schemes DP130101265 and DP150100003.

#### REFERENCES

[1] T.Q. Wang, C. He, J. Armstrong, "Angular Diversity for Indoor MIMO Optical Wireless Communications," in Proc. IEEE International Conference on Communications (ICC2015), London, UK, Jun 2015.

[2] C. Yang, H.-R. Shao, "WiFi-Based Indoor Positioning," IEEE Communications Magazine, Vol 53, No 3, Mar 2015, pp. 150-157.

[3] R. Faragher, R. Harle, "Location Fingerprinting with Bluetooth Low Energy Beacons," IEEE Journal on Selected Areas in Communications, DOI: 10.1109/JSAC.2015.2430281.

[4] S. Gezici, Z. Tian, G.B. Giannakis, H. Kobayashi, A.F. Molisch, H.V. Poor, Z. Sahinoglu, "Localization via Ultra-Wideband Radios," IEEE Signal Processing Magazine, Jul 2005, pp. 70-84.

[5] J. Armstrong, Y. A. Sekercioglu and A. Neild, "Visible Light Positioning: A Roadmap for International Standardisation," IEEE Communications Magazine, Vol 51, No 12, Dec 2013, pp. 68-73.

[6] T. Komine, M. Nakagawa, "Performance Evaluation of Visible-Light Wireless Communication System Using White LED Lightings," in Proc. 9th Symposium on Computers and Communications (ISCC2004), Alexandria, Egypt, Jun 2004, pp. 258-263.

[7] S.-Y. Jung, S. Hann, C.-S. Park, "TDOA-Based Optical Wireless Indoor Localization Using LED Ceiling Lamps," IEEE Transactions on Consumer Electronics, Vol 57, No 4, Nov 2011, pp. 1592-1597.

[8] K. Panta, J. Armstrong, "Indoor Localization Using White LEDs," Electronics Letters, Vol 48, No 4, Feb 2012, pp. 228-230.

[9] S. Hann, J.-H. Kim, S.-Y. Jung, C.-S. Park, "White LED Ceiling Lights Positioning Systems for Optical Wireless Indoor Applications," in Proc. ECOC 2010, Torino, Italy, Sep 2010.

[10] M. Rahaim, G.B. Prince, T.D.C. Little, "State Estimations and Motion Tracking for Spatially Diverse VLC Networks," in Proc. Globecom Workshops, Anaheim, CA, USA, Dec 2012, pp. 1249-1253.

[11] H.-S. Kim, D.-R. Kim, S.-H. Yang, Y.-H. Son, S.-K. Han, "An Indoor Visible Light Communication Positioning System Using a RF Allocation Technique," Journal of Lightwave Technology, Vol 31, No 1, Jan 2013, pp. 134-144.

[12] S.-H. Yang, H.-S. Kim, Y.-H. Son, and S.-K. Han, "Three-Dimensional Visible Light Indoor Localization Using AOA and RSS With Multiple Optical Receivers," Journal of Lightwave Technology, Vol 32, No 14, Jul 2014, pp. 2480-2485.

[13] G. Kail, P. Maechler, N. Preyss, A. Burg, "Robust Asynchronous Indoor Localization Using LED Lighting," IEEE International Conference on Acoustics, Speech and Signal Processing (ICASSP2014), Florence, Italy, May 2014.

[14] A.N. Simonov, "Cramer-Rao Bounds in Functional Form: Theory and Application to Passive Optical Ranging," Journal of the Optical Society of America A, Vol 31, No 12, 2014, pp. 2680-2693.

[15] X. Zhang, J. Duan, Y. Fu, A. Shi, "Theoretical Accuracy Analysis of Indoor Visible Light Communication Positioning System Based on Received Signal Strength Indicator," Journal of Lightwave Technology, Vol 32, No 21, Nov 2014, pp. 3578-3584.

[16] A. Sahin, Y.S. Eroglu, I. Guvenc, N. Pala, M. Yuksel, "Hybrid 3D Localization for Visible Light Communication Systems," submitted to Journal of Lightwave Technology, arxiv.org/pdf/1508.05776.

[17] T.Q. Wang, Y.A. Sekercioglu, A. Neild, J. Armstrong, "Position Accuracy of Time-of-Arrival Based Ranging Using Visible Light with Application in Indoor Localization Systems," Journal of Lightwave Technology, Vol 31, No 20, Oct 2013, pp. 3302-3308.

[18] H.L. Van Trees, "Detection, Estimation, and Modulation Theory," New York, NY, USA, Wiley, 1968.

[19] J.M. Kahn, J.R. Barry, "Wireless Infrared Communications," Proceedings of the IEEE, Vol 85, No 2, Feb 1997, pp. 265-298.

[20] L. Zeng, D.C. O'Brien, H.L. Minh, G.E. Faulkner, K. Lee, D. Jung, Y. Oh, E.T. Wong, "High Data Rate Multiple Input Multiple Output (MIMO) Optical Communications Using White LED Lighting," IEEE Journal on Selected Areas in Communications, Vol 27, No 9, Dec 2009, pp. 1654-1662.